DMD Fast Forward. Published on June 30, 2006 as doi:10.1124/dmd.106.009977

DMD #9977

Title:

Characterization of the rhesus monkey CYP3A64 enzyme: Species comparisons of CYP3A substrate specificity and kinetics using baculovirus-expressed recombinant enzymes

Authors:

Brian Carr, Ryan Norcross, Yulin Fang, Ping Lu, A. David Rodrigues, Magang Shou, Tom Rushmore, and Catherine Booth-Genthe

Institutions:

Department of Drug Metabolism, Merck Research Laboratories, West Point, Pennsylvania (BC, RN, YF, PL, MS, TR); Drug Metabolism and Pharmacokinetics, Bristol-Myers Squibb, New Jersey (ADR); Department of Drug Metabolism, Amgen, Thousand Oaks, CA (CBG)

DMD Fast Forward. Published on June 30, 2006 as DOI: 10.1124/dmd.106.009977
This article has not been copyedited and formatted. The final version may differ from this version.

Running Title:

Characterization of rhesus CYP3A64

Address Correspondence to:

Dr. Brian A. Carr, Preclinical Drug Metabolism, WP75A-203, West Point, PA 19486.

Phone: 215-652-7128, Fax: 215-652-2410, E-mail: brian_carr@merck.com

The Number of:

Text pages: 32

Tables: 5

Figures: 7

References: 41

The number of words in Abstract: 192

Introduction: 744

Discussion: 1433

Abbreviations:

CYP or P450 – cytochrome P450; bp – base pairs; 7-benzoxy-4-trifluoromethylcoumain – BFC;

7-hydroxy-4-trifluoromethylcoumarin – HFC

ABSTRACT:

The rhesus monkey (*Macaca mulatta*) is a primate species used extensively as a preclinical safety species in drug development. In this report, we describe the cloning, expression, and characterization of CYP3A64 (AY334551), a CYP3A4 homolog expressed in rhesus liver. The deduced amino acid sequence was found to be 93% similar to human CYP3A4, 83% similar to human CYP3A5, and identical to the previously reported cynomolgus monkey CYP3A8 (Komori et al., 1992). The substrate specificity of CYP3A64 for testosterone (0-250 μM), midazolam (0-200 μM), nifedipine (0-200μM), and BFC (0-200 μM) were compared with recombinant enzymes from rat (CYP3A1, CYP3A2), dog (CYP3A12, CYP3A26), rabbit (CYP3A6), and human (CYP3A4, CYP3A5). Immuno- and chemical-inhibition of CYP3A64 was demonstrated using the inhibitory monoclonal antibody MAb 10-1-1 (anti-3A4) and ketoconazole (0-10 μM). The utility of CYP3A64 to be used as a standard in monkey induction assays was shown and the concentration of CYP3A64 protein in rhesus liver microsomes was estimated to be 72 pmol/mg protein. In summary, these results support the utilization of rhesus monkey CYP3A64 for *in vitro* drug metabolism studies and provide a more complete understanding of CYP3A substrate specificities and species differences in metabolic capabilities.

Introduction

Cytochrome P450s (CYP or P450) are a superfamily of enzymes involved in the elimination of a wide variety of chemical xenobiotics including pharmaceuticals, carcinogens, and environmental pollutants (Wrighton and Stevens, 1992). CYP3A4 is the most abundant of these enzymes in humans and responsible for the biotransformation of nearly 50% of all pharmaceuticals (Guengerich, 1995). Substrates for CYP3A4 include such structurally distinct molecules as testosterone, nifedipine, lidocaine, lovastatin, erythromycin, cyclosporine, diazepam, midazolam, and coumarins.

Rhesus monkeys (*Macaca mulatta*) and cynomolgus monkeys (*Macaca fascicularis*) are widely used throughout pharmaceutical industry as preclinical safety species. Much emphasis is placed on the overall drug safety profile and the extrapolated CYP3A metabolic activities of monkeys to corresponding human drug metabolism variables, even though very little information is known about monkey CYP3A enzymes or their metabolic capabilities. There are relatively few reports, compared to rat and human, regarding the specific activity of rhesus and cynomolgus monkey CYP3A enzyme activities, and most of these reports are from purified regenerated systems or liver homogenates and not from recombinantly expressed enzyme systems (Ohta et al., 1989; Ohmori et al., 1993; Ramana and Kohli, 1999; Matsunaga et al., 2002). Although it is believed that monkey CYP3A metabolic capabilities should be similar to human CYP3A, there has not been an in-depth investigation of the enzymatic properties of the individual monkey CYP3A isoforms. Therefore we sought to clone, express, and characterize the major CYP3A4-like drug metabolizing enzyme from rhesus monkey liver.

Based on its predicted homology to human CYP3A4, we cloned the CYP3A4 homolog from rhesus monkeys. The cloned cDNA was expressed using a commonly used insect cell

expression system and characterized with multiple probe substrates. Insect cells offer several advantages over other expression systems: (1) they do not require alteration of the P450 coding sequence for expression, (2) they lack endogenous cytochrome P450s and (3) they can be used to make microsomes or co-expressed with NADPH-P450 oxidoreductase (OR) to produce 'supersomes' (Gonzalez and Korzekwa, 1995; Crespi and Miller, 1999).

It is valuable to understand the metabolic capabilities of preclinical animal models to accurately predict safety and clearance profiles of pharmaceutical candidates in development. Therefore, in addition to the evaluation of the rhesus CYP3A64 enzyme activity in relationship to the human CYP3A4 enzyme, a species comparison was performed using recombinant enzymes from Beagle dogs, Sprague-Dawley rats, and New Zealand rabbits. These comparisons should be valuable for interpreting results from preclinical models.

Other methods for investigating the physiological fate of pharmaceutical candidates involves the use of chemical and immunological inhibition techniques that investigate the contribution of a particular drug metabolizing enzyme toward the biotransformation of a compound of interest. These tools, for example, can be used to determine whether a preclinical candidate is a potential CYP3A inhibitor. Inhibition of CYP3A is a major liability for a compound in development due to the potential for adverse drug-drug interactions. Further understanding of *in vitro-in vivo* correlations in monkeys and other preclinical animal species, will allow more confident predictions of human *in vivo* outcomes from *in vitro* data. To explore the use of recombinant rhesus CYP3A64 for these types of assays, we investigated whether a common CYP3A4 chemical inhibitor, ketoconazole, and a CYP3A4 inhibitory monoclonal antibody, MAb 10-1-1 (Mei et al., 1999), would be effective at inhibiting CYP3A64 present in

rhesus liver microsomes and compare the results obtained from similar studies with human liver microsomes.

Pharmaceuticals frequently elicit CYP enzyme induction, which is a problem for adequate exposure to the active pharmaceutical, both for efficacy and for achieving appropriate exposures during safety evaluation. Induction causes drug-drug interactions by increasing the elimination of other co-administered drugs which can result in failed efficacy or increased metabolite exposure. For this reason, a compound's potential to induce CYP enzymes is screened for during drug development. In the case of determining rhesus induction, we investigated the utilization of the recombinant CYP3A64 protein as a standard for immunological detection of rhesus CYP3A64 enzyme using the anti-human CYP3A4 antibody. This characteristic will allow for the determination of CYP3A64 in rhesus tissue samples and subcellular preparations. Furthermore, by cloning the CYP3A64 cDNA we will be able to design quantitative PCR primers and probes for measuring changes in RNA expression.

Data reported in this manuscript provides useful information regarding rhesus monkey CYP3A metabolic capabilities. The similarity of rhesus CYP3A64 enzyme to the homologous human CYP3A4 enzyme was demonstrated and the usefulness of the recombinant CYP3A64 enzyme in typical *in vitro* assays employed during the drug development process was explored.

Methods and Materials

Materials. Novex mini-gel system, 10% Bis-Tris precast gels (1.5mm, 15 wells), PVDF membranes, NuPage LDS sample buffer (4X), NuPage reducing agent (10X), NuPage MOPS running buffer (20X), NuPage antioxidant, NuPage transfer buffer (20X), MagicMark Western protein standards, and Benchmark pre-stained protein ladder were purchased from Invitrogen (Carlsbad, CA). Supersignal West Femto maximum sensitivity substrate kit was purchased from Pierce (Rockford, IL). All chemicals including midazolam, triazolam, cortisone, NAPDH, and ketoconazole were purchased from Sigma-Aldrich (St. Louis, MO). Testosterone and 6β-hydroxytestosterone were obtained from Steraloids (Wilton, NH). Pooled male human liver microsomes (Lot# 0310241) and rhesus monkey liver microsomes (Lot# 0310189) were purchased from Xenotech (Lenexa, KS). Recombinant enzymes CYP3A4, CYP3A12, CYP3A26, CYP3A1, CYP3A6, as well as MAb 10-1-1 (anti-CYP3A4) were generated in-house at Merck Research Labs (West Point, PA). Nifedipine, oxidized nifedipine, 7-benzoxy-4-trifluoromethylcoumain (BFC), 7-hydroxy-4-trifluoromethylcoumarin (HFC), recombinant CYP3A4, CYP3A5, and CYP3A2 where purchased from BD Gentest (Woburn, MA). All molecular biology reagents, restriction enzymes, pFastBac vectors, Cellfectin reagent, Sf21 insect cells (*Spodoptera frugiperda* Sf21) and Sf-900 II SFM (serum-free medium) were obtained from Invitrogen (Carlsbad, CA).

Cloning of rhesus CYP3A64. The cDNA for rhesus CYP3A64 was obtained by amplification of mRNA prepared from male rhesus liver (sample obtained from Laboratory Animal Resources, Merck Research Laboratories, West Point, PA). The primary cDNA transcripts were generated by reverse transcription using Superscript II (Invitrogen) and oligo-$(dT)_{12\text{-}18}$ according to the manufacturer's recommendations. PCR amplification of the target

cDNAs were performed using Platinum *pfx* polymerase (Invitrogen) with the forward (5-AGA TAA GGA AGG AAA GTA GTG ATG-3) and reverse (5-AGC AGA AGT CCT TAG TAA AAT TCA-3) primers designed against consensus sequences of cynomolgus monkey, human, and rabbit CYP3A genes. The PCR products were cloned into pCR2.1 (Invitrogen) and the DNA sequence was confirmed by sequencing, using the Big Dye Terminator cycle sequencing kit, and analyzed on an ABI Prism 310 Genetic Analyzer (Applied Biosystems, Foster City, CA). The deduced sequence for CYP3A64 was sent to Dr. David Nelson (University of Tennessee, Memphis, TN) for appropriate nomenclature and then deposited in GenBank (accession number AY334551).

Heterologous expression of CYP3A64 in Sf21 cells. PCR amplification of CYP3A64 cDNA was performed using forward and reverse primers to engineer SpeI and XhoI restriction sites for cloning into the pFastBac vector. Recombinant baculovirus containing the entire coding region of rhesus CYP3A64 was generated using the BAC-to-BAC baculovirus expression system (Invitrogen) according to the manufacturer's specifications. A "high-titer" virus was generated by 3 rounds of amplification and collected when cell viability reached 50%. Spectrally active P450 expression (Omura and Sato, 1964) was optimized by performing several co-infections of CYP3A64 and human P450 oxidoreductase recombinant baculovirus. Sf21 cell media was supplemented with 1 µg of hemin per ml of medium in the form of a hemin-albumin complex.

Microsomal preparation of CYP3A64. After 72 hours cells were collected by centrifugation and microsomal preparations were performed (Shou et al., 2003). Microsomes were prepared by differential centrifugation at two speeds (9,000 and 110,000 x g). Insect cells were separated from media by pelleting cells at 4,000 rpm for 10 min. Cell pellets were resuspended in 20% glycerol in 0.1 M potassium phosphate (KPi) buffer (pH 7.5) and sonicated

with two 20 sec bursts at 70% power at -4ºC. The sonicated lysate was centrifuged at 9,000 x g for 15 min to pellet the S9 fraction. The supernatant was then centrifuged at 110,000 x g for 70 min to collect the microsomal pellet. The supernatant (cytosol) was discarded and the microsomal pellet was resuspended with 0.1 M sucrose, 1.15% KCl, 0.5 mM DTT, 1 mM EDTA, in 0.1 M KPi buffer (pH 7.5). P450 concentration was measured using the CO-difference spectrum (Omura and Sato, 1964) and co-expressed P450 oxidoreductase (OR) activity was determined using the cytochrome *c* reduction assay (Vermilion and Coon, 1978). Protein content was calculated using Bio-Rad's Bradford assay. Microsomes were stored at -70ºC until used.

Western Blot Analysis of rhesus CYP3A64. The specificity of the monoclonal antibody, MAb 10-1-1, for rhesus CYP3A64 was analyzed by using the Western blotting standard protocol from Invitrogen's NuPage technical guide and PVDF membranes. The primary antibody was incubated overnight at a dilution of 1:500 in blocking solution (25 mM Tris-HCl, 150 mM NaCl) containing 5% dried milk. The secondary antibody, goat anti-mouse HRP (2-10 ng/mL), was diluted 1:5000 and incubated for 1 hr in the same blocking solution. Blots were analyzed using an Alpha Innotech digital CCD camera with Alpha Ease FC software version 3.2.3 (San Leandro, CA).

Metabolism of CYP3A substrates. Incubation mixtures of proteins with testosterone, midazolam, nifedipine, and BFC were prepared in 96-deep well formats with 0.2 mL final volumes. All incubations were performed in duplicate at linear conditions determined previously (data not shown): testosterone (0-240 µM) incubated for 10 min, midazolam (0-200 µM) for 5 min, nifedipine (0-200 µM) for 10 min, and BFC (0-200 µM) for 10 min. Incubation mixtures containing the listed substrates were prepared at 4ºC and contained 5 pmol of recombinant

enzymes or 100 µg of liver microsomes protein, 0.1 M KPi buffer (pH = 7.5), and 1 mM $MgCl_2$. The samples were preincubated for 3 min at 37ºC in a shaking water bath, then the reaction was initiated by addition of 1 mM NADPH. After the indicated incubation times, the reactions were terminated by addition of 2 volumes acetonitrile containing 600 ng/mL of the appropriate internal standard: cortisone (for testosterone), triazolam (for midazolam), and nimodipine (for nifedipine). Samples were centrifuged at 4,000 rpm for 10 min to pellet precipitated proteins and membranes. The supernatants were transferred to another 96-well plate for drying. Samples were dried under nitrogen stream at 37ºC and resuspended in 100 µL of 25% acetonitrile in 0.1% formic acid. For BFC the reaction was terminated by adding 1 volume of 4:1 acetonitrile:0.5 M Tris Base solution and transferring 100 µL to a black 96-well plate. Quantitation of HFC was determined using a Spectra Max Gemini (Molecular Devices, Sunnyvale, CA) fluorometer with excitation/emission settings 409/530 nm using SOFTmax PRO v3.1.1 software. Controls and standard curves for each reference metabolite (6β-OH testosterone, 1′-OH midazolam, oxidized nifedipine, and HFC) were performed using identical conditions.

Testosterone, Midazolam, and Nifedipine LC-MS/MS analysis. Quantitative analysis of testosterone metabolites was determined by LC-MS/MS. Instrumentation consisted of Perkin Elmer Series 200 LC pumps and LEAP autosampler coupled to a Sciex API 2000 mass spectrometer operated in positive ion mode. Samples of 20 µL were chromatographed using a Agilent Zorbax SB-C18 (5 µm, 4.6 mm x 75 mm; Agilent Technologies, Palo Alto, CA) with a mobile phase consisting of solvent A (90% water/10% methanol/0.05% formic acid) and solvent B (10% water/90% acetonitrile/0.05% formic acid). Samples were eluted over 10 min using a gradient of 75% solvent A to 40% solvent A from 0.1 to 7 min, returning to 75% solvent A at 7.1 min until 10 min, at a flow rate of 0.75 mL/min. This gradient was essential to separate 6β-OH

testosterone from the numerous hydroxylated testosterone peaks. Metabolites and internal standard were detected under atmospheric pressure chemical ionization (APCI) conditions and identified using the transitions *m/z* 305.5 → 269 (6β-hydroxytestosterone) and *m/z* 361 → 163.2 (cortisone). The rate of 6β-hydroxytestosterone was determined using a standard curve determined concurrently.

The hydroxylation of midazolam was determined using the same LC-MS/MS system used for analysis of testosterone hydroxylation. Samples were chromatographed using an ACE 5 µm C18 column (Advanced Chromatography Technologies, Bridge of Don, Aberdeen, UK) with a mobile phase consisting of solvent A (90% water/10% methanol/0.05% formic acid) and solvent B (10% water/90% acetonitrile/0.05% formic acid). Samples of 10 µL were eluted over 3 min using a gradient of 90% solvent A to 20% solvent A from 0.1-2.5 min returning to 90% solvent by 2.6 min with a flow rate of 1.5 mL/min. Metabolites 1'-OH MDZ and 4-OH MDZ were detected under positive APCI and identified using the *m/z* 342.1 → 203 (1'-OH MDZ), *m/z* 342.1 → 234.1 (4-OH MDZ), and *m/z* 343.1 → 308.1 (triazolam) transitions. A standard curve for 1'-OH MDZ was used to determine the production of 1'-OH MDZ and estimate the production of 4-OH MDZ.

The oxidation of nifedipine was quantified using the LC-MS/MS system described above. The samples were chromatographed using a Discovery HS C18 (5 µm; 5 cm x 2.1 mm; Supelco, Sigma-Aldrich Co., St. Louis, MO) with a mobile phase consisting of the same solvent A and B from above. Reconstituted samples of 20 µL were separated over 4 min at 1.2 mL/min using a gradient of 80% A to 55% A from 0.2-3 min to 20% A at 3.5 min returning to 80% A by 3.6 min. Oxidized nifedipine was determined under positive APCI using the *m/z* transition of 344.9 → 284 and nimodipine the internal standard at *m/z* 419.1 → 343.2.

DMD Fast Forward. Published on June 30, 2006 as DOI: 10.1124/dmd.106.009977
This article has not been copyedited and formatted. The final version may differ from this version.

Kinetic Analysis. Curve fitting was performed to determine kinetic parameters using classic and atypical kinetic equations (Segal, 1975). Equations were selected by goodness of fit based on R^2 values and least residual sum of squares (RSS). K_m or S_{50} and V_{max} were calculated by fitting data to either the Michaelis-Menton ($v = V_{max}[S]/K_m+[S]$) or Hill ($v = V_{max}[S]^n/(S_{50}+[S]^n)$) equations using non-linear regression analysis and SigmaPlot 7.1 (SPSS Science, Chicago, IL). Substrate inhibition for midazolam data analysis were fit using $v = V_{max}[S]/K_m+[S]+K_m[S]^2/K_i$. Chemical inhibition was determined using % = Min + Max-Min/$(1+I/Ki)^n$.

Chemical Inhibition of CYP3A64. The inhibitory capacity of the prototypical chemical inhibitor ketoconazole was used to compare the human CYP3A4 and rhesus CYP3A64 enzymes. Testosterone (50 µM) was co-incubated with varying concentrations (0-10 µM) of ketoconazole using the enzyme reaction conditions described earlier. Samples were processed and percent inhibition of 6β-OH testosterone formation relative to control (without ketoconazole) was assessed using the LC-MS/MS method described earlier.

Immuno-inhibition of CYP3A64. To determine the inhibitory activity of human monoclonal antibody (MAb 10-1-1) against rhesus CYP3A64, 10 µL of ascites/mL of incubation (or diluted ascites containing inhibitory antibody) were added to the 0.2 mL testosterone incubations described above. Antibody was added to the reaction mixture and pre-incubated for 5 min before addition of testosterone (50 µM). Samples were brought to 37ºC for 4 min then reaction was initiated by addition of NADPH (1 mM). Samples were processed and analyzed for 6β-OH testosterone.

Results

Cloning and Sequencing of rhesus CYP3A64. Total liver RNA was isolated from a small tissue sample of rhesus monkey (*Macaca mulatta*) liver and used to generate total cDNA by reverse transcription with oligo$(dT)_{12\text{-}18}$. The resulting cDNA was subsequently used, along with primers designed against consensus CYP3A, in a PCR reaction to generate a product that was subcloned for sequencing. Several individually-purified plasmid DNA molecules were sequenced and CYP3A64 was identified. A variant sequence CYP3A64v1 was also identified during our screening. Both CYP3A64 and CYP3A64v1 have been reconfirmed in liver samples from additional rhesus monkeys (data not shown), although CYP3A64v1 was not present in all samples. Figure 1 shows the nucleotide and deduced amino acid sequence for rhesus CYP3A64 and CYP3A64v1. The cDNA of CYP3A64 is 1512 bp and codes for a protein 504 amino acids in length. CYP3A64 and CYP3A64v differ by 1 bp at position 878 (T→A) resulting in a leucine to glutamate (L293Q) amino acid change. Although CYP3A64v was not characterized in these studies, this variant may have some relevance since a variant at the same location in the human CYP3A4 gene has been described (Dai et al., 2001). The human variant CYP3A4 enzyme (CYP3A4*18) is different, however, in that it has a T→C nucleotide change, which results in a leucine to proline (L298P) amino acid change. CYP3A4*18 was identified in Chinese and Japanese populations (Yamamoto et al., 2003; Hu et al., 2005), while the expressed enzyme was shown to have increased testosterone activity (Dai et al., 2001). In the future it may be interesting to characterize and compare the rhesus CYP3A64v (L293Q) identified.

Comparisons of the percent identity of the deduced protein sequences and nucleotide sequences from several CYP3A species are presented in Table 1. CYP3A64 (AY334551) differs from CYP3A8 (Komori et al., 1992) by 2 bp at positions 147 and 807. Neither of these

differences alters the amino acid sequence; therefore, the rhesus and cynomolgus monkey CYP3A enzymes are identical. The human proteins, CYP3A4 and CYP3A5 are 93% and 83% similar to the rhesus CYP3A64 at the amino acid level, respectively. The high similarity to CYP3A4 supports the notion that CYP3A64 and CYP3A8 are the rhesus and cynomolgus homologs of CYP3A4. Several CYP3A proteins from other species are also listed with each sharing 70-77% sequence similarity to CYP3A64. As expected the monkey species share considerable similarity to the human and less similarity to other commonly studied preclinical animal species.

Heterologous expression of CYP3A64 in Sf21 cells. The restriction enzyme sites for SpeI and XhoI were engineered into the cDNA of CYP3A64 using PCR for subsequent subcloning into the pFastBac vector (pFB). The newly constructed pFB-3A64 vector was used in the Bac-to-Bac™ system to generate a recombinant bacmid molecule. The bacmid DNA was then used to transfect plated Sf21 cells to generate a recombinant baculovirus, which was amplified by three successive rounds to make a "high-titer" baculovirus for expression studies. Co-infection of Sf21 cells with the CYP3A64 baculovirus and a previously generated baculovirus carrying the redox partner enzyme NADPH-P450 oxidoreductase (OR) was optimized by monitoring for spectrally active P450 expression. An archetypal cytochrome P450 spectrum was obtained for CYP3A64 with an absorbance maximum at 448 nm. Cytochrome c reduction was also monitored and expression studies were optimized to obtain an OR to P450 molar ratio of 3:1. The optimized co-infected Sf21 cells were subsequently used to prepare supersomes to characterize the recombinant CYP3A64 enzyme.

Testosterone Kinetics using Recombinant CYP3A Enzymes. The most commonly used *in vitro* probe for CYP3A activity is 6β-hydroxylation of testosterone (Walsky and Obach, 2004)

(Kenworthy et al., 1999). Figure 2 compares the metabolism data for 6β-hydroxylation of testosterone catalyzed by human CYP3A4 and CYP3A5 with the metabolism data from rhesus CYP3A64. CYP3A4, CYP3A5, and CYP3A64 enzymes all showed sigmoidal or autoactivation kinetics for testosterone 6β-hydroxylation with Hill coefficients of n = 1.3, n = 2.1, and n = 1.1, respectively (see Table 2). CYP3A64 was fit to a sigmoidal kinetic model for consistency, however it showed negligible autoactivation by testosterone (n = 1.1). The goodness of fit (R^2 = 0.9971 and RSS = 10.27) was very similar to the fit (R^2 = 0.9964 and RSS = 5.56) from the classic Michaelis-Menton equation. The V_{max} value for 6β-hydroxylation of testosterone by CYP3A4 (39.7 nmol/nmol P450/min) was higher than CYP3A64 (28.2 nmol/nmol P450/min), but this had only a minor effect on the *in vitro* intrinsic clearance value CL_{int} (V_{max}/S_{50}), 1.6 compared to 1.1 mL/nmol P450/min. The S_{50} of testosterone for CYP3A64 and CYP3A4 were similar 25.3 vs 24.7 μM, respectively. In contrast, CYP3A5 had a lower affinity for testosterone (S_{50} = 74.7 μM) and lower V_{max} (19.2 nmol/nmol P450/min) for a much lower CL_{int} value (0.26 mL/nmol P450/min), roughly 6-fold. This difference highlights the known difference between CYP3A4 and CYP3A5 for 6β-hydroxylation of testosterone (Williams et al., 2002; Patki et al., 2003) and shows that CYP3A64 is structurally and enzymatically more similar to CYP3A4.

Several CYP3A recombinant enzymes from species used frequently in preclinical drug development were compared for 6β-hydroxylase activity. All enzymes displayed autoactivation or sigmoidal kinetics and kinetic parameters were determined using Hill's equation for sigmoidal kinetics (Table 2). The rat CYP3A2 recombinant enzyme preparation appeared to be most active based on the *in vitro* intrinsic clearance value CL_{int} of 3.3 versus CYP3A4 (1.6), CYP3A64 (1.1), CYP3A6 (0.3), CYP3A12 (0.2), CYP3A1 (0.1), and CYP3A26 (<0.1), which is largely due to the affinity of CYP3A2 for testosterone (S_{50} = 5.8 μM). However, CYP3A2 supersomes were

from a commercial source and expressed with cytochrome b5, which may augment the activity compared to the in-house preparations (Yamazaki et al., 1996; Yamazaki et al., 1999). Although the addition of b5 has been shown to be somewhat substrate and isoform specific (Nakajima et al., 2002; Yamazaki et al., 2002), and may not be an issue in our studies, the possibility of cytochrome b5 to potentially enhance the enzymatic properties of CYP3A2 is noteworthy and will be an issue for all the kinetics determined in this report. Determining the effect of cytochrome b5 on these enzymes was beyond the target of these studies.

Midazolam Kinetics using Recombinant CYP3A Enzymes. The hydroxylation of midazolam has become a widely used model for the determination of CYP3A activity *in vitro* and *in vivo* (Thummel and Wilkinson, 1998). Midazolam metabolism by CYP3A enzymes has improved properties over testosterone metabolism in that it has fewer metabolites and can be administered to patients to look at *in vivo* CYP3A activity. It is hydroxylated by CYP3A enzymes at the 1′-position and 4-position. The 1′-hydroxylation of midazolam by CYP3A enzymes is the major pathway and the *in vitro* comparison of CYP3A64 and CYP3A4 is demonstrated in Figure 3. CYP3A64 and CYP3A4 were highly susceptible to midazolam substrate inhibition at midazolam concentrations greater than 10 µM. Therefore, a substrate inhibition model was used to fit the data presented in Figure 3. Complete kinetic parameters for the 1′-hydroxylation of midazolam by all recombinant enzymes are listed in Table 3. Both CYP3A64 and CYP3A4 had similar affinity for midazolam, evident by K_m values of 1.4 µM and 1.9 µM, respectively. However, CYP3A64 appeared more active based on the V_{max} value for midazolam 1′-hydroxylation of 6.2 nmol/nmol P450/min compared to the CYP3A4 V_{max} value of 4.7 nmol/nmol P450/min. Each enzyme was susceptible to substrate inhibition with a K_i of 306 µM for CYP3A64 and 383 µM for CYP3A4. Overall, CYP3A64 had higher midazolam 1′-

hydroxylation activity than CYP3A4 based on the CL_{int} value of 4.3 mL/nmol P450/min and 2.6 mL/nmol P450/min, respectively. Comparisons with other CYP3A enzymes showed that all enzymes tested had comparable midazolam kinetics, except CYP3A26 and CYP3A6. CYP3A26 had a low V_{max} value and significantly higher K_m value of 98.3 μM compared to the other CYP3A enzymes which had K_m values in low μM range, whereas CYP3A6 had a comparable K_m with a low V_{max} value. CYP3A12, CYP3A2, and CYP3A1 V_{max} values ranged from 4.0-5.8 nmol/nmol P450/min and K_m values ranged from 0.9-2.0 μM. Taken together, these studies demonstrate that midazolam is a very good *in vitro* probe substrate for CYP3A64 and will likely be a good *in vivo* substrate to investigate induction and drug-drug interaction potential in rhesus monkeys.

Nifedipine Kinetics using Recombinant CYP3A Enzymes. Another structurally distinct molecule, nifedipine, has been shown to be oxidized by CYP3A enzymes (Williams et al., 2002; Patki et al., 2003; Walsky and Obach, 2004). Figure 4 demonstrates the rate of oxidized nifedipine formation following incubation of CYP3A4 and CYP3A64 with increasing concentrations of nifedipine (0-60 μM). Substrate concentrations higher than 60 μM caused substantial substrate inhibition and were not used to calculate enzyme kinetics for CYP3A4 and CYP3A64. Both CYP3A4 and CYP3A64 showed activation kinetics for nifedipine oxidation and were analyzed using Hill's sigmoidal kinetic model (Table 4). Hill coefficient's for CYP3A64 and CYP3A4 were n = 1.4 and n = 1.6, respectively. CYP3A64 was twice as active in oxidizing nifedipine as CYP3A4 based on CL_{int} values of 2.4 mL/nmol P450/min compared to 1.2 mL/nmol P450/min. Incubations of other recombinant CYP3A enzymes with varying concentrations of nifedipine (0-60 μM) were performed as described in the methods. All CYP3A enzymes tested from the various species were capable of catalyzing nifedipine oxidation

DMD Fast Forward. Published on June 30, 2006 as DOI: 10.1124/dmd.106.009977
This article has not been copyedited and formatted. The final version may differ from this version.

with S_{50} values ≤ 22 µM. Unlike CYP3A4 and CYP3A64, CYP3A2, CYP3A1, CYP3A26, and CYP3A6 did not follow activation kinetics and were fit using Michaelis-Menton equation. Out of all the enzymes tested, dog CYP3A26 and rabbit CYP3A6 were the least effective at nifedipine oxidation, primarily due to low V_{max} values. Dog CYP3A12 displayed significant substrate inhibition. The substrate inhibition was pronounced and began at concentrations > 7.5 µM; therefore, the dog CYP3A12 data was fit using a substrate inhibition equation and a K_i of 38 µM was determined.

BFC Kinetics using Recombinant CYP3A Enzymes and Liver Microsomes. High-throughput screening of CYP3A inhibition is a common procedure in drug development (Stresser et al., 2002). Fluorescent probe substrates, such as BFC, that do not require liquid chromatography or mass spectral analysis for quantitation are useful tools for these types of routine screenings. Figure 5 shows the metabolism data for the generation of HFC by CYP3A4, CYP3A5, and CYP3A64. Each enzyme displayed sigmoidal kinetics for the generation of HFC, thus Hill's equation was utilized for calculation of kinetic parameters. CYP3A64 was 2-fold more active at metabolizing BFC than CYP3A4 and 5-fold more active than CYP3A5 based on CL_{int}. Table 5 lists all the calculated kinetic parameters for all the tested CYP3A enzymes. By far, CYP3A64 was the most active enzyme for dealkylating BFC. Interestingly, all enzymes had similar S_{50} values whereas the V_{max} values ranged from 0.1-23.0 nmol/nmol P450/min with CYP3A4 and CYP3A64 having much larger values compared to the other isoforms. Activation was significant with Hill's constant (n) values ranging from 1.4-2.2.

Inhibition of CYP3A64 enzymatic activity. Selective inhibitors, such as ketoconazole, and monoclonal antibodies that are capable of selectively inhibiting a particular enzymatic reaction are extremely useful for characterizing the metabolic pathway or fate of a new drug. Figure 6

(A) demonstrates the effect of the ketoconazole on 6β-hydroxylation of testosterone catalyzed by CYP3A64 and CYP3A4 and their corresponding liver microsome preparations. The inhibition of enzymatic activity by ketoconazole is nearly identical for CYP3A64 (IC_{50} = 0.1 μM) as it is for CYP3A4 (IC_{50} = 0.1 μM). Furthermore, the inhibitory effect of ketoconazole on rhesus and human liver microsomes supports that CYP3A64 and CYP3A4 are the principle testosterone 6β-hydroxylating enzymes, since the IC_{50} of ketoconazole in these systems were 0.1 μM and <0.1 μM, respectively. These values are highly comparable to the corresponding individual isoforms.

Monoclonal antibodies are extremely valuable tools for phenotyping the principle P450 enzymes responsible for the biotransformation of a new drug candidate. There are many options and reagents available which have varying degrees of potency and specificity. We utilized a highly selective mouse anti-human CYP3A4 monoclonal antibody (MAb 10-1-1) for our routine phenotyping studies, which we developed in-house for the inhibition of CYP3A-mediated reactions (Mei et al., 1999). Figure 6 (B) demonstrates the % inhibition of testosterone 6β-hydroxylation of CYP3A4, CYP3A64, rhesus liver microsomes, and human liver microsomes by increasing concentrations of MAb 10-1-1 compared to control mouse ascites. The CYP3A4 specific inhibitory monoclonal antibody MAb 10-1-1 was a potent inhibitor of rhesus CYP3A64 and human CYP3A4 enzymes with complete inhibition attainable with 5 μL of antibody/mL incubation. In addition, the antibody completely inhibited the 6β-hydroxylation of testosterone in both rhesus and human liver microsomes at comparable concentrations.

Western Blotting Analysis of rhesus CYP3A64 Protein. Induction of drug metabolizing enzymes by drugs is of concern due to the potential for decreased drug exposures and drug-drug interactions. Induction is measured in multiple ways, but usually involves measuring changes in mRNA, enzyme marker assays, or protein levels by immunological

techniques. First to support the selectivity of our monoclonal antibody for CYP3A64, we demonstrated the binding of MAb 10-1-1 for CYP3A64 and compared the binding to equal amounts (0.1 pmol) of other CYP3A enzymes (Figure 7, A). MAb 10-1-1 shows comparable binding efficiency for CYP3A64 and CYP3A4 with a slight interaction to CYP3A5 and no binding to CYP3A12, CYP3A26, CYP3A1, CYP3A2, and CYP3A6. Secondly we investigated whether MAb 10-1-1 and CYP3A64 could be used to estimate the amount of CYP3A64 present in rhesus liver microsomes. In Figure 7 (B), a standard curve was generated by hybridization of MAb 10-1-1 to increasing amounts of CYP3A64 (0.1-2 pmol). This data was used to generate an equation to estimate the amount of CYP3A64 present in a commercially available rhesus liver microsome preparation (Figure 7, C). The intensity of the detected band was determined and used to calculate a CYP3A64 content of 72 pmol/mg microsomal protein. Using the same equations the CYP3A4 content was calculated to be 33 pmol/mg microsomal protein. Similar standard curves were generated using CYP3A4 and the results were indistinguishable (data not shown). Based on the quantitation of the total P450/mg protein reported by the manufacturer of these liver microsome preparations, the CYP3A4 and CYP3A64 proteins represent a P450 content of 8% and 5% of total, respectively. These values appears to be underestimated based on literature reports of the abundance of CYP3A proteins in rhesus or in relation to human (Stevens et al., 1993; Shimada et al., 1994).

Discussion

The pharmaceutical industry is required to investigate the potential toxicity of new drug candidates in nonrodent species, usually dog or monkey, due to differences in metabolism and physiological functions between rodents and man. For this, Beagle dogs and rhesus or cynomolgus monkeys have been used for many years. To ensure that these animal species are exposed to adequate drug levels, including the numerous metabolites that are generated in human tissues, drug metabolism studies utilizing dog and monkey liver microsomes and hepatocytes preparations are used routinely. Findings from such studies are used to predict the animal PK parameters and metabolite profile of the drug candidate. Furthermore, data from these preclinical animal studies are often extrapolated to predict the human exposure and clearance of a new drug candidate. Yet despite the extensive application of these studies, until recently, few studies have been performed with the isolated or expressed cytochrome P450 enzymes responsible for these biotransformations in preclinical test species (Shou et al., 2003).

In this report we presented the cloning and characterization of CYP3A64, which we propose is the rhesus homolog of the major human drug metabolizing enzyme CYP3A4. CYP3A64 was cloned from rhesus liver tissue and is 100% identical at the amino acid level and 99% identical at the mRNA sequence to the previously cloned CYP3A8 from cynomolgus monkey (Komori et al., 1992). Both enzymes are highly similar to the human enzyme sharing 93% amino acid identity. It has been shown that CYP3A8 represents ~20% of the P450 in monkey liver (Ohmori et al., 1993), which compares with the proportion of CYP3A4 found in human liver (Burke et al., 1994). The finding that CYP3A64 and CYP3A8 are identical at the amino acid level is encouraging because it suggests that both of these species may exhibit highly similar CYP3A-mediated drug clearance characteristics.

Rhesus monkey metabolic functions have been compared to humans and found to be highly similar (Stevens et al., 1993; Sharer et al., 1995). Although overall capacity has been shown to be greater in monkey, this has been largely attributed to increased enzyme levels and not necessarily substrate selectivity or enzyme activity (Ohmori et al., 1993; Stevens et al., 1993; Sharer et al., 1995). Metabolic studies from these and others characterizing monkey P450s seem to show that monkey P450s are very similar to human P450s in enzymatic preference, but apparent differences in substrate affinities or enzyme levels generally yield higher activities in monkeys. Furthermore, the similarity of rhesus and cynomolgus monkeys, both of which are from the same genus, would allow either of these monkey species to be used as preclinical models for human studies.

It is widely believed that two or more probe reactions for CYP3A4-based drug interactions must be investigated and although testosterone 6β-hydroxylation and midazolam 1′-hydroxylation are the most common reactions, oxidation of nifedipine and dealkylation of coumarin-based molecules are also widely tested (Yuan et al., 2002). The reasons behind this requisite are largely due to the wide substrate binding site and diverse molecular structures the enzyme is able to metabolize. Based on chemical inhibition studies and substrate-activity correlations, there are at least two distinct substrate groups (Kenworthy et al., 1999; Stresser et al., 2000). To ascertain whether CYP3A64 shared this CYP3A4 substrate preference, in this report we investigated the functional activity of CYP3A64 towards four, commonly used, structurally distinct CYP3A probe substrates. Furthermore, to determine whether there were any significant species differences with rhesus we compared CYP3A64 to CYP3A enzymes from human, dog, rat, and rabbit.

CYP3A enzymes are known to display non-hyperbolic kinetics (Ueng et al., 1997; Korzekwa et al., 1998; Shou et al., 1999; Domanski et al., 2001) for many substrates. In our studies, testosterone, nifedipine, and BFC oxidations displayed autoactivation or sigmoidal kinetics for all tested CYP3A enzymes. This non-hyperbolic behavior is proposed to reflect more than one molecule binding to the active site leading to activation (Korzekwa et al., 1998; Domanski et al., 2001). In addition to activation, most of the recombinant enzymes were subject to substrate inhibition at very high concentrations. Midazolam hydroxylation was most affected with substrate inhibition appearing at very low concentrations. This substrate inhibition of midazolam hydroxylation by increasing midazolam concentrations has been reported previously for CYP3A enzymes (Kronbach et al., 1989; Gorski et al., 1994). Despite this significant inhibition, midazolam is one of the most widely used substrates to probe *in vitro* and *in vivo* CYP3A activity (Ghosal et al., 1996; Williams et al., 2002; Patki et al., 2003). Yet it appears that midazolam hydroxylation, as a probe, is mostly used at lower concentrations before substrate inhibition occurs. In general, midazolam was a sensitive probe substrate for the CYP3A enzymes we tested. Dog CYP3A12 was the most active enzyme for midazolam 1′-hydroxylation with a CL_{int} value of 6.3 mL/nmol P450/min. Rhesus CYP3A64, rat CYP3A1, human CYP3A4, and rat CYP3A2 were also strongly active at midazolam hydroxylation with CL_{int} values ranging from 2.0-4.3 mL/nmol P450/min. Dog CYP3A26 and rabbit CYP3A6 were different with CL_{int} values of 0.1 mL/nmol P450/min and 0.9 mL/nmol P450/min, respectively. The substrate inhibition for CYP3A64, CYP3A4, CYP3A12, CYP3A1, and CYP3A2 was abrupt leading to strong inhibition at concentrations >10 μM. CYP3A26, on the other hand, did not display substrate inhibition with increasing midazolam concentrations. It has been demonstrated that two midazolam metabolites, 1′-OH and 4-OH, are generated from

CYP3A-mediated oxidations (Kronbach et al., 1989; Gorski et al., 1994). The formation of these two metabolites has been proposed to result from the binding of midazolam at two separate sites in CYP3A4 (Khan et al., 2002) and that the enzyme inactivation occurs at the 1′-OH position. Schrag et al., 2001 proposed that the CYP3A4 biotransformation of triazolam, a close structural analog of midazolam, also behaves as a two-site model and substrate inhibition results from competition between the two sites for reactive oxygen (Schrag and Wienkers, 2001). Furthermore, Wang et al., found that testosterone inhibits 1′-OH midazolam formation and activates 4-OH midazolam formation (Wang et al., 2000). For simplicity and comparative purposes, in our studies, we used the simpler substrate inhibition model to compare the catalytic efficiencies of the various CYP3A isoforms for midazolam. The formation of 4-OH midazolam was observed in these studies (data not shown) yet it was not analyzed due to lack of an appropriate standard and since saturation of the formation was rarely observed. However, superficial analysis of the kinetics revealed a biphasic kinetic pattern for the formation of 4-OH midazolam, which would also lend credit to the proposal of two distinct binding sites. The elucidation of the mechanisms of 1′-OH midazolam versus 4-OH midazolam was beyond the scope of these studies, but warrants further investigation.

It was demonstrated that the rhesus CYP3A64 enzyme and rhesus liver microsomes were subject to chemical inhibition using the CYP3A specific chemical inhibitor ketoconazole with IC_{50} values in the 0.1 μM range. Antibody mediated inhibition is a powerful, highly-selective, means to inhibit CYP3A activity in a microsomal incubation. Immuno-inhibition of CYP3A activity is used routinely to determine the role of CYP3A in xenobiotic metabolism. The CYP3A4 specific inhibitory monoclonal antibody (MAb 10-1-1) was a potent inhibitor of rhesus and human CYP3A enzymes with complete inhibition attainable with 5 μL of antibody/mL

incubation. It was not surprising, but fortunate, that despite the high selectivity of monoclonal antibodies, MAb 10-1-1 was as potent at CYP3A64 as it was for CYP3A4 at inhibiting testosterone hydroxylation. The selectivity of MAb 10-1-1 was demonstrated and used to estimate the content of rhesus CYP3A64 enzyme in rhesus liver microsomes at 72 pmol/mg total protein. This is an estimate as we currently are unaware of the contribution of other rhesus CYP3A enzymes in rhesus liver. These studies also do not rule out the possibility of this antibody cross-reacting with other proteins in rhesus microsomes; however based on the specificity of monoclonal antibodies and demonstration of the selectivity, it gives us confidence that at least the antibody can be used to detect and inhibit CYP3A proteins in rhesus microsomes. In general, it seems from our studies that using recombinantly expressed enzymes to accurately determine P450 protein levels in microsomes may underestimate the P450 present in microsomal preparations. This underestimation may be the result of spectral quantitation of P450 in protein preparations from expression systems where the enzyme is largely over-expressed. Spectral determination of P450 will not take into account immunoreactive spectrally-inactive protein, thereby creating a standard curve which underestimates the amount of protein present in the microsome preparation.

It has been demonstrated that rhesus monkeys have higher CYP3A immunoreactive protein, which contributes to an apparent increased metabolic activity (Stevens et al., 1993). Based on our immunodetection studies, CYP3A64 levels alone do not appear to account for the observed 6- to 11-fold increased activity observed in those studies, but perhaps the combination of increased enzyme activity and slightly higher protein levels may account for the changes. Otherwise it would suggest that other CYP3A enzymes may have overlapping substrate

specificity. Future studies should include the determination of the specificity and contribution of other rhesus CYP3A enzymes to CYP3A-mediated reactions.

Through our comparisons, it was found that rhesus CYP3A64 was most similar to human CYP3A4 when compared to the activities of the other CYP3A recombinant enzymes CYP3A5, CYP3A12, CYP3A26, CYP3A1, CYP3A2, and CYP3A6. This data should provide useful information on CYP3A-mediated metabolism in commonly used preclinical test species and supports the role of species specific drug metabolizing enzymes in drug development.

Acknowledgments

The authors would like to acknowledge Dr. Thomayant Prueksaritanont for her patience and contributions to this area of research. We would also like to acknowledge Qin Mei for her efforts towards the generation of the highly selective monoclonal antibody used in these studies.

References

Burke MD, Thompson S, Weaver RJ, Wolf CR and Mayer RT (1994) Cytochrome P450 specificities of alkoxyresorufin O-dealkylation in human and rat liver. *Biochem Pharmacol* **48:**923-936.

Crespi CL and Miller VP (1999) The use of heterologously expressed drug metabolizing enzymes--state of the art and prospects for the future. *Pharmacol Ther* **84:**121-131.

Dai D, Tang J, Rose R, Hodgson E, Bienstock RJ, Mohrenweiser HW and Goldstein JA (2001) Identification of variants of CYP3A4 and characterization of their abilities to metabolize testosterone and chlorpyrifos. *J Pharmacol Exp Ther* **299:**825-831.

Domanski TL, He YA, Khan KK, Roussel F, Wang Q and Halpert JR (2001) Phenylalanine and tryptophan scanning mutagenesis of CYP3A4 substrate recognition site residues and effect on substrate oxidation and cooperativity. *Biochemistry* **40:**10150-10160.

Ghosal A, Satoh H, Thomas PE, Bush E and Moore D (1996) Inhibition and kinetics of cytochrome P4503A activity in microsomes from rat, human, and cdna-expressed human cytochrome P450. *Drug Metab Dispos* **24:**940-947.

Gonzalez FJ and Korzekwa KR (1995) Cytochromes P450 expression systems. *Annu Rev Pharmacol Toxicol* **35:**369-390.

Gorski JC, Hall SD, Jones DR, VandenBranden M and Wrighton SA (1994) Regioselective biotransformation of midazolam by members of the human cytochrome P450 3A (CYP3A) subfamily. *Biochem Pharmacol* **47:**1643-1653.

Guengerich FP (1995) Human Cytochrome P450 Enzymes, in: *Cytochrome P450: Structure, Mechanism, and Biochemistry* (Ortiz de Montellano P ed), pp 377-530, Plenum Press, New York.

Hu YF, He J, Chen GL, Wang D, Liu ZQ, Zhang C, Duan LF and Zhou HH (2005) CYP3A5*3 and CYP3A4*18 single nucleotide polymorphisms in a Chinese population. *Clin Chim Acta* **353:**187-192.

Kenworthy KE, Bloomer JC, Clarke SE and Houston JB (1999) CYP3A4 drug interactions: correlation of 10 in vitro probe substrates. *Br J Clin Pharmacol* **48:**716-727.

Khan KK, He YQ, Domanski TL and Halpert JR (2002) Midazolam oxidation by cytochrome P450 3A4 and active-site mutants: an evaluation of multiple binding sites and of the metabolic pathway that leads to enzyme inactivation. *Mol Pharmacol* **61:**495-506.

Komori M, Kikuchi O, Sakuma T, Funaki J, Kitada M and Kamataki T (1992) Molecular cloning of monkey liver cytochrome P-450 cDNAs: similarity of the primary sequences to human cytochromes P-450. *Biochim Biophys Acta* **1171:**141-146.

Korzekwa KR, Krishnamachary N, Shou M, Ogai A, Parise RA, Rettie AE, Gonzalez FJ and Tracy TS (1998) Evaluation of atypical cytochrome P450 kinetics with two-substrate models: evidence that multiple substrates can simultaneously bind to cytochrome P450 active sites. *Biochemistry* **37:**4137-4147.

Kronbach T, Mathys D, Umeno M, Gonzalez FJ and Meyer UA (1989) Oxidation of midazolam and triazolam by human liver cytochrome P450IIIA4. *Mol Pharmacol* **36:**89-96.

Matsunaga T, Iwawaki Y, Komura A, Watanabe K, Kageyama T and Yamamoto I (2002) Monkey hepatic microsomal alcohol oxygenase: purification and characterization of a cytochrome P450 enzyme catalyzing the stereoselective oxidation of 7alpha- and 7beta-hydroxy-delta8-tetrahydrocannabinol to 7-oxo-delta8-tetrahydrocannabinol. *Biol Pharm Bull* **25:**42-47.

Mei Q, Tang C, Assang C, Lin Y, Slaughter D, Rodrigues AD, Baillie TA, Rushmore TH and Shou M (1999) Role of a potent inhibitory monoclonal antibody to cytochrome P-450 3A4 in assessment of human drug metabolism. *J Pharmacol Exp Ther* **291:**749-759.

Nakajima M, Tane K, Nakamura S, Shimada N, Yamazaki H and Yokoi T (2002) Evaluation of approach to predict the contribution of multiple cytochrome P450s in drug metabolism using relative activity factor: effects of the differences in expression levels of NADPH-cytochrome P450 reductase and cytochrome b(5) in the expression system and the differences in the marker activities. *J Pharm Sci* **91:**952-963.

Ohmori S, Horie T, Guengerich FP, Kiuchi M and Kitada M (1993) Purification and characterization of two forms of hepatic microsomal cytochrome P450 from untreated cynomolgus monkeys. *Arch Biochem Biophys* **305:**405-413.

Ohta K, Kitada M, Hashizume T, Komori M, Ohi H and Kamataki T (1989) Purification of cytochrome P-450 from polychlorinated biphenyl-treated crab-eating monkeys: high homology to a form of human cytochrome P-450. *Biochim Biophys Acta* **996:**142-145.

Omura T and Sato R (1964) The carbon monoxide-binding pigment of liver microsomes. I. Evidence for its hemoprotein nature. *J Biol Chem* **239:**2370-2378.

Patki KC, Von Moltke LL and Greenblatt DJ (2003) In vitro metabolism of midazolam, triazolam, nifedipine, and testosterone by human liver microsomes and recombinant cytochromes p450: role of cyp3a4 and cyp3a5. *Drug Metab Dispos* **31:**938-944.

Ramana KV and Kohli KK (1999) Purification and characterization of the hepatic CYP2C and 3A isozymes from phenobarbitone pretreated rhesus monkey. *Mol Cell Biochem* **198:**79-88.

Schrag ML and Wienkers LC (2001) Triazolam substrate inhibition: evidence of competition for heme-bound reactive oxygen within the CYP3A4 active site. *Adv Exp Med Biol* **500:**347-350.

Segal I (1975) *Enzyme Kinetics: Behavior and Analysis of Rapid Equilibrium and Steady-State Enzyme Systems*. John Wiley and Sons, Inc., New York.

Sharer JE, Shipley LA, Vandenbranden MR, Binkley SN and Wrighton SA (1995) Comparisons of phase I and phase II in vitro hepatic enzyme activities of human, dog, rhesus monkey, and cynomolgus monkey. *Drug Metab Dispos* **23:**1231-1241.

Shimada T, Yamazaki H, Mimura M, Inui Y and Guengerich F (1994) Interindividual variations in human liver cytochrome P-450 enzymes involved in the oxidation of drugs, carcinogens and toxic chemicals: studies with liver microsomes of 30 Japanese and 30 Caucasians. *J Pharmacol Exp Ther* **270:**414-423.

Shou M, Mei Q, Ettore MW, Jr., Dai R, Baillie TA and Rushmore TH (1999) Sigmoidal kinetic model for two co-operative substrate-binding sites in a cytochrome P450 3A4 active site:

an example of the metabolism of diazepam and its derivatives. *Biochem J* **340 (Pt 3):**845-853.

Shou M, Norcross R, Sandig G, Lu P, Li Y, Lin Y, Mei Q, Rodrigues AD and Rushmore TH (2003) Substrate specificity and kinetic properties of seven heterologously expressed dog cytochromes p450. *Drug Metab Dispos* **31:**1161-1169.

Stevens JC, Shipley LA, Cashman JR, Vandenbranden M and Wrighton SA (1993) Comparison of human and rhesus monkey in vitro phase I and phase II hepatic drug metabolism activities. *Drug Metab Dispos* **21:**753-760.

Stresser DM, Blanchard AP, Turner SD, Erve JC, Dandeneau AA, Miller VP and Crespi CL (2000) Substrate-dependent modulation of CYP3A4 catalytic activity: analysis of 27 test compounds with four fluorometric substrates. *Drug Metab Dispos* **28:**1440-1448.

Stresser DM, Turner SD, Blanchard AP, Miller VP and Crespi CL (2002) Cytochrome P450 fluorometric substrates: identification of isoform-selective probes for rat CYP2D2 and human CYP3A4. *Drug Metab Dispos* **30:**845-852.

Ueng YF, Kuwabara T, Chun YJ and Guengerich FP (1997) Cooperativity in oxidations catalyzed by cytochrome P450 3A4. *Biochemistry* **36:**370-381.

Vermilion JL and Coon MJ (1978) Identification of the high and low potential flavins of liver microsomal NADPH-cytochrome P-450 reductase. *J Biol Chem* **253:**8812-8819.

Walsky RL and Obach RS (2004) Validated assays for human cytochrome P450 activities. *Drug Metab Dispos* **32:**647-660.

Wang RW, Newton DJ, Liu N, Atkins WM and Lu AY (2000) Human cytochrome P-450 3A4: in vitro drug-drug interaction patterns are substrate-dependent. *Drug Metab Dispos* **28:**360-366.

Williams JA, Ring BJ, Cantrell VE, Jones DR, Eckstein J, Ruterbories K, Hamman MA, Hall SD and Wrighton SA (2002) Comparative metabolic capabilities of CYP3A4, CYP3A5, and CYP3A7. *Drug Metab Dispos* **30:**883-891.

Wrighton SA and Stevens JC (1992) The human hepatic cytochromes P450 involved in drug metabolism. *Crit Rev Toxicol* **22:**1-21.

Yamamoto T, Nagafuchi N, Ozeki T, Kubota T, Ishikawa H, Ogawa S, Yamada Y, Hirai H and Iga T (2003) CYP3A4*18: it is not rare allele in Japanese population. *Drug Metab Pharmacokinet* **18:**267-268.

Yamazaki H, Nakajima M, Nakamura M, Asahi S, Shimada N, Gillam EM, Guengerich FP, Shimada T and Yokoi T (1999) Enhancement of cytochrome P-450 3A4 catalytic activities by cytochrome b(5) in bacterial membranes. *Drug Metab Dispos* **27:**999-1004.

Yamazaki H, Nakamura M, Komatsu T, Ohyama K, Hatanaka N, Asahi S, Shimada N, Guengerich FP, Shimada T, Nakajima M and Yokoi T (2002) Roles of NADPH-P450 reductase and apo- and holo-cytochrome b5 on xenobiotic oxidations catalyzed by 12 recombinant human cytochrome P450s expressed in membranes of Escherichia coli. *Protein Expr Purif* **24:**329-337.

Yamazaki H, Nakano M, Imai Y, Ueng YF, Guengerich FP and Shimada T (1996) Roles of cytochrome b5 in the oxidation of testosterone and nifedipine by recombinant

cytochrome P450 3A4 and by human liver microsomes. *Arch Biochem Biophys* **325:**174-182.

Yuan R, Madani S, Wei XX, Reynolds K and Huang SM (2002) Evaluation of cytochrome P450 probe substrates commonly used by the pharmaceutical industry to study in vitro drug interactions. *Drug Metab Dispos* **30:**1311-1319.

Figure Captions

Figure 1. The nucleotide and predicted amino acid sequence of the complete translated regions of the rhesus CYP3A64 and CYP3A64v cDNAs. The amino acids are represented by their three-letter codes beneath each codon. The sequence of CYP3A64v is shown where it differs from the sequence of CYP3A64 by italics above the sequence.

Figure 2. The mean velocity data for the 6β-hydroxylation of testosterone catalyzed by human CYP3A4 (●), human CYP3A5 (▼), and rhesus CYP3A64 (○) are presented. Data and regression analysis demonstrate the activation or sigmoidal kinetics and similarity of the CYP3A4 and CYP3A64 enzyme activities. The details of the reaction are described under *Methods*. The solid lines through the experimental data shows the best fit for the linear regression analysis using the Hill equation ($v = V_{max}[S]^n/(S_{50}+[S]^n)$ for sigmoidal kinetics. v = nmol 6β-OH testosterone/nmol P450/min; S = testosterone (μM).

Figure 3. The mean velocity data for the 1′-hydroxylation of midazolam catalyzed by human CYP3A4 (●) and rhesus CYP3A64 (○) are presented. The data demonstrates a model for substrate inhibition kinetics and reveals the resemblance between the two enzymes. The details of the reaction are described under *Methods*. The solid lines through the experimental data shows the best fit for the linear regression analysis using a substrate inhibition model ($v = V_{max}[S]/K_m+[S]+ K_m[S]^2/K_i$). v = nmol 1′-OH midazolam/nmol P450/min; S = midazolam (μM).

Figure 4. The metabolism data for the oxidation of nifedipine by human CYP3A4 (●) and rhesus CYP3A64 (○) are presented. Data and regression analysis show sigmoidal kinetics and

demonstrate the similarity between the CYP3A4 and CYP3A64 enzyme activities. The details of the nifedipine oxidation reaction are described under *Methods*. The solid lines through the experimental data shows the best fit for the linear regression analysis using the Hill equation ($v = V_{max}[S]^n/(S_{50}+[S]^n)$) for sigmoidal kinetics. v = nmol oxidized nifedipine/nmol P450/min; S = nifedipine (μM).

Figure 5. The metabolism data for the dealkylation of BFC by human CYP3A4 (●), human CYP3A5 (▼), and rhesus CYP3A64 (○) are presented. Data and regression analysis demonstrate sigmoidal kinetics and comparison of the CYP3A4, CYP3A5, and CYP3A64 enzyme activities. The reaction conditions for BFC are described under *Methods*. The solid lines through the experimental data shows the best fit for the linear regression analysis using the Hill equation ($v = V_{max}[S]^n/(S_{50}+[S]^n)$) for sigmoidal kinetics. v = nmol HFC/nmol P450/min; S = BFC (μM).

Figure 6. (A) Chemical inhibition of human liver microsomes (●), CYP3A4 (○), rhesus liver microsomes (▼), and CYP3A64 (Δ) catalyzed 6β-hydroxylation of testosterone activity by ketoconazole. The reaction conditions for ketoconazole inhibition are described under *Methods*. Data are presented as % inhibition of 6β-hydroxytestosterone formation with increasing concentrations of ketoconazole and plotted on a logarithmic scale to determine the IC_{50} (μM). The absolute catalytic activities, at 50 μM testosterone, in these studies were 23.3 nmol/nmol P450/min for CYP3A64, 2.0 nmol/mg protein/min for rhesus liver microsomes, 28.2 nmol/nmol P450/min for CYP3A4, and 2.0 nmol/mg protein/min for human liver microsomes. (B) Immuno-inhibition of human liver microsomes (●), CYP3A4 (○), rhesus liver microsomes (▼),

and CYP3A64 (Δ) catalyzed 6β-hydroxytestosterone formation by an anti-CYP3A4 specific monoclonal antibody (MAb 10-1-1). The reaction conditions for immuno-inhibition are described under *Methods*. Data are presented as % inhibition of 6β-OH testosterone formation with increasing amounts of MAb 10-1-1. The absolute catalytic activities at 50 μM testosterone in the control ascites were 21.8 nmol/nmol P450/min for CYP3A64, 2.24 nmol/mg protein/min for rhesus liver microsomes, 29.8 nmol/nmol P450/min for CYP3A4, and 2.3 nmol/mg protein/min for human liver microsomes.

Figure 7. (A) The specificity of anti-CYP3A4 monoclonal antibody (MAb 10-1-1) for rhesus CYP3A64 and human CYP3A4 over human CYP3A5, dog CYP3A12 and CYP3A26, rat CYP3A1 and CYP3A2, and rabbit CYP3A6 (0.1 pmol of each enzyme). The Western blotting conditions are detailed under *Methods*. Analysis revealed immunoreactive proteins at approximately 54 kDa. (B) The use of recombinantly expressed CYP3A64 for the immuno-quantification of CYP3A64 in rhesus liver microsomes. The immuno-quantitation procedures are described under *Methods*. (C) A standard curve using increasing amounts of recombinant CYP3A64 (0.1-2.0 pmol) was used to generate an equation to predict the amount of CYP3A64 immunoreactive protein in rhesus liver microsomes. Data estimates 72 pmol/mg total protein of rhesus CYP3A64. R – 10 μg of rhesus liver microsomes; H – 10 μg of human liver microsomes; CYP3A4 – 1 pmol; Con – Insect control microsomes.

DMD Fast Forward. Published on June 30, 2006 as DOI: 10.1124/dmd.106.009977
This article has not been copyedited and formatted. The final version may differ from this version.

Table 1. Sequence comparisons between CYP3A64 and other cytochrome P450s from the CYP3A subfamily[a].

Cytochrome P450[b]	Species	Protein (% Identity)	Nucleotide (% Identity)
CYP3A8	Cynomolgus Monkey	100	99
CYP3A4	Human	93	95
CYP3A5	Human	83	88
CYP3A12	Beagle Dog	77	82
CYP3A26	Beagle Dog	75	82
CYP3A2	Sprague-Dawley Rat	70	76
CYP3A1	Sprague-Dawley Rat	71	76
CYP3A6	New Zealand White Rabbit	74	80

[a] The amino acid sequence of CYP3A64 was aligned with other members of the CYP3A subfamily and the percent identity was calculated using CLUSTALW (http://www.ebi.ac.uk/clustalw/).

[b] Amino acid sequences for the various CYP3A enzymes were obtained from Entrez, the database search and retrieval system at NCBI (http://www.ncbi.nlm.nih.gov).

DMD Fast Forward. Published on June 30, 2006 as DOI: 10.1124/dmd.106.009977
This article has not been copyedited and formatted. The final version may differ from this version.

Table 2. Enzyme kinetic parameters for the hydroxylation of testosterone by recombinant CYP3A enzymes.

	Testosterone 6β-hydroxylation			
Enzyme	V_{max} [a]	S_{50} [b]	CL_{int} [c]	n [d]
CYP3A64	28.2 ± 0.7	25.3 ± 1.9	1.1	1.1
CYP3A4	39.7 ± 0.8	24.7 ± 1.5	1.6	1.3
CYP3A5	19.2 ± 0.9	74.7 ± 4.7	0.3	2.1
CYP3A12	10.7 ± 0.4	51.1 ± 3.5	0.2	1.5
CYP3A26	1.2 ± 0.1	31.2 ± 4.0	<0.1	1.2
CYP3A2	19.0 ± 0.2	5.8 ± 0.2	3.3	1.2
CYP3A1	2.1 ± 0.3	43.9 ± 11.7	0.1	1.4
CYP3A6	9.6 ± 1.2	28.6 ± 10.5	0.3	1.0

S_{50} and V_{max} were calculated by fitting data to the Hill ($v = V_{max}[S]^n/(S_{50}+[S]^n)$) equation using non-linear regression analysis and SigmaPlot 7.1 (SPSS Science, Chicago, IL).

[a] V_{max} = nmol/nmol P450/min for recombinant enzymes

[b] S_{50} = μM testosterone

[c] CL_{int} = *in vitro* clearance value (V_{max}/S_{50})

[d] n = Hill coefficient

Table 3. Enzyme kinetic parameters for the hydroxylation of midazolam by recombinant CYP3A enzymes.

	Midazolam 1'-hydroxylation			
Enzyme	V_{max} [a]	K_m [b]	CL_{int} [c]	K_i [d]
CYP3A64	6.2 ± 0.2	1.4 ± 0.2	4.3	306 ± 44
CYP3A4	4.7 ± 0.2	1.9 ± 0.2	2.6	383 ± 46
CYP3A12	5.8 ± 0.2	0.9 ± 0.1	6.3	117 ± 19
CYP3A26	0.6 ± 0.0	98.3 ± 14.1	<0.1	NA
CYP3A2	4.0 ± 0.2	2.0 ± 0.3	2.0	167 ± 23
CYP3A1	5.1 ± 0.3	1.2 ± 0.2	4.2	41 ± 5
CYP3A6	0.8 ± 0.0	0.9 ± 0.1	0.9	100 ± 32

K_m and V_{max} were calculated by fitting data to a substrate inhibition model ($v = V_{max}[S]/K_m+[S]+K_m[S]^2/K_i$) equation using non-linear regression analysis and SigmaPlot 7.1 (SPSS Science, Chicago, IL).

[a] V_{max} = nmol/nmol P450/min

[b] K_m = μM midazolam

[c] CL_{int} = *in vitro* clearance value (V_{max}/S_{50})

[d] K_i = μM midazolam

DMD Fast Forward. Published on June 30, 2006 as DOI: 10.1124/dmd.106.009977
This article has not been copyedited and formatted. The final version may differ from this version.

Table 4. Enzyme kinetic parameters for the oxidation of nifedipine by recombinant CYP3A enzymes.

	Nifedipine oxidation				
Enzyme	V_{max} [a]	S_{50} / K_m [b]	CL_{int} [c]	n [d]	K_i [e]
CYP3A64	9.3 ± 0.3	3.9 ± 0.3	2.4	1.4	
CYP3A4	6.2 ± 0.1	5.3 ± 0.3	1.2	1.6	
CYP3A12	0.8 ± 0.1	0.8 ± 0.2	1.0		38 ± 8
CYP3A26	0.6 ± 0.1	12.7 ± 2.7	0.1		
CYP3A2	9.1 ± 0.3	11.1 ± 0.9	0.8		
CYP3A1	6.3 ± 0.4	22.0 ± 3.2	0.3		
CYP3A6	0.9 ± 0.1	21.3 ± 3.0	<0.1		

S_{50} and V_{max} were calculated by fitting data to the Hill ($v = V_{max}[S]^n/(S_{50}+[S]^n)$) equation using non-linear regression analysis and SigmaPlot 7.1 (SPSS Science, Chicago, IL).

[a] V_{max} = nmol/nmol P450/min for recombinant enzymes

[b] S_{50}/K_m = μM nifedipine

[c] CL_{int} = *in vitro* clearance value (V_{max}/S_{50})

[d] n = Hill coefficient

Table 5. Enzyme kinetic parameters for the dealkylation of BFC by recombinant CYP3A enzymes.

	BFC dealkylation			
Enzyme	V_{max} [a]	S_{50} [b]	CL_{int} [c]	n [d]
CYP3A64	23.0 ± 0.6	10.6 ± 0.7	2.2	1.7
CYP3A4	12.6 ± 0.4	13.5 ± 1.2	0.9	2.1
CYP3A5	3.9 ± 0.1	11.0 ± 0.6	0.4	2.2
CYP3A12	2.9 ± 0.1	13.2 ± 1.2	0.2	1.7
CYP3A26	0.4 ± 0.0	10.9 ± 0.3	<0.1	2.0
CYP3A2	3.6 ± 0.1	13.1 ± 0.9	0.3	2.1
CYP3A1	2.0 ± 0.1	9.4 ± 1.2	0.2	1.4
CYP3A6	0.1 ± 0.0	16.0 ± 2.9	<0.1	1.7

S_{50} and V_{max} were calculated by fitting data to the Hill ($v = V_{max}[S]^n/(S_{50}+[S]^n)$) equation using non-linear regression analysis and SigmaPlot 7.1 (SPSS Science, Chicago, IL).

[a] V_{max} = nmol/nmol P450/min for recombinant enzymes

[b] S_{50} = μM BFC

[c] CL_{int} = *in vitro* clearance value (V_{max}/S_{50})

[d] n = Hill coefficient

DMD Fast Forward. Published on June 30, 2006 as DOI: 10.1124/dmd.106.009977
This article has not been copyedited and formatted. The final version may differ from this version.

Figure 1

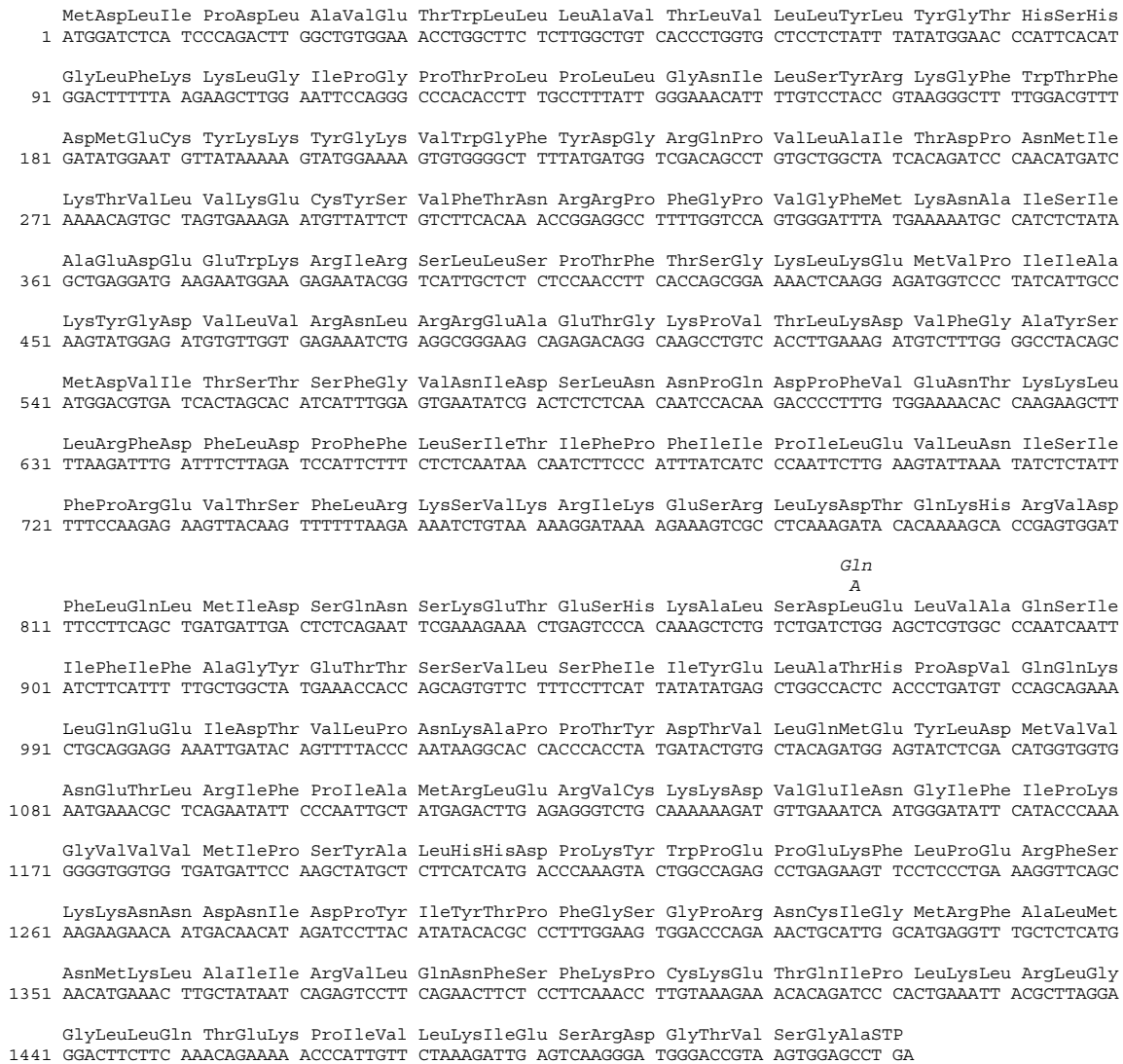

DMD Fast Forward. Published on June 30, 2006 as DOI: 10.1124/dmd.106.009977
This article has not been copyedited and formatted. The final version may differ from this version.

Figure 2

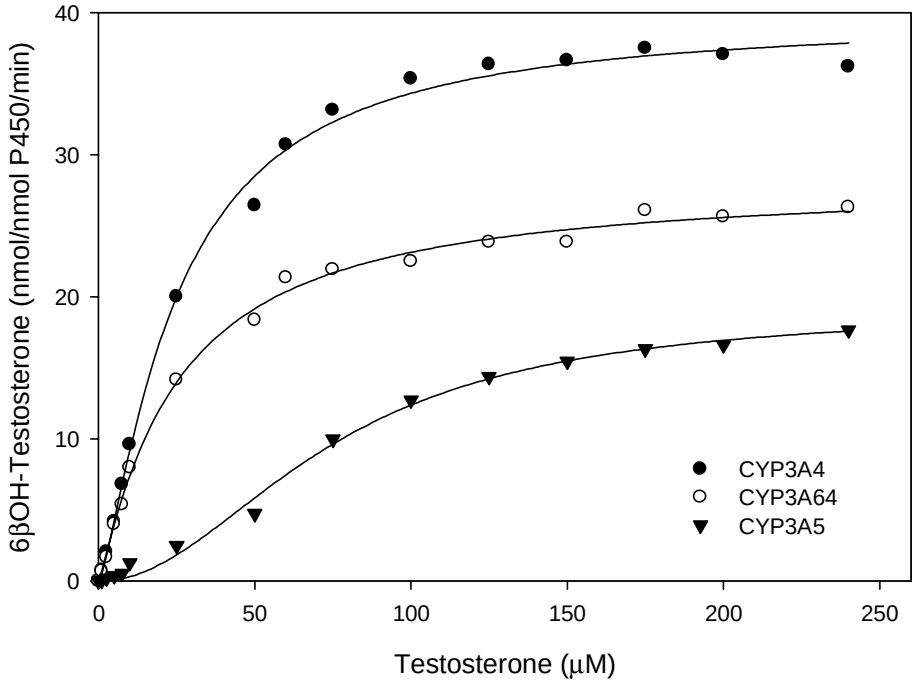

DMD Fast Forward. Published on June 30, 2006 as DOI: 10.1124/dmd.106.009977
This article has not been copyedited and formatted. The final version may differ from this version.

Figure 3

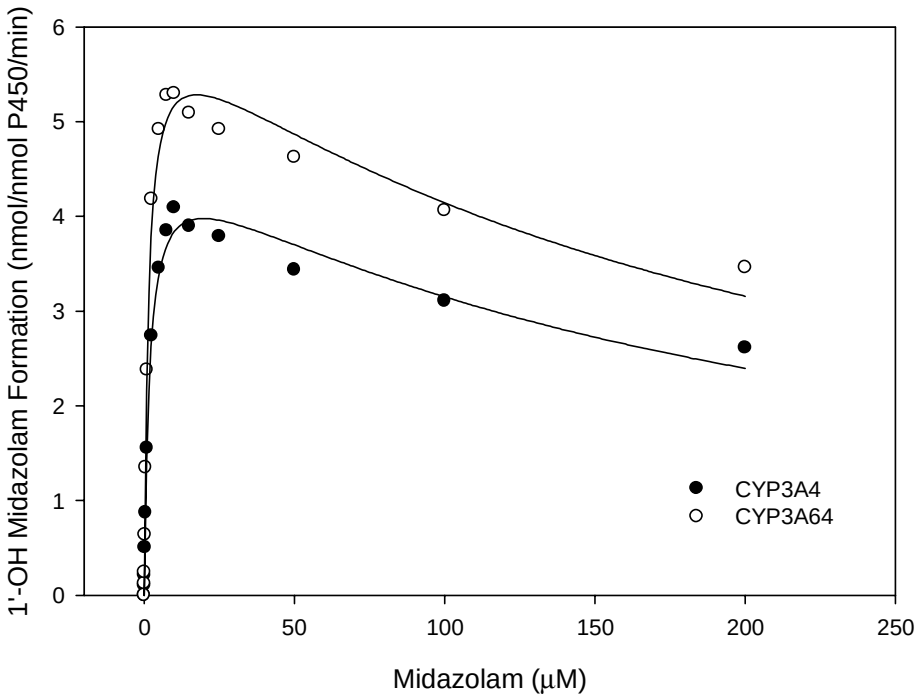

DMD Fast Forward. Published on June 30, 2006 as DOI: 10.1124/dmd.106.009977
This article has not been copyedited and formatted. The final version may differ from this version.

Figure 4

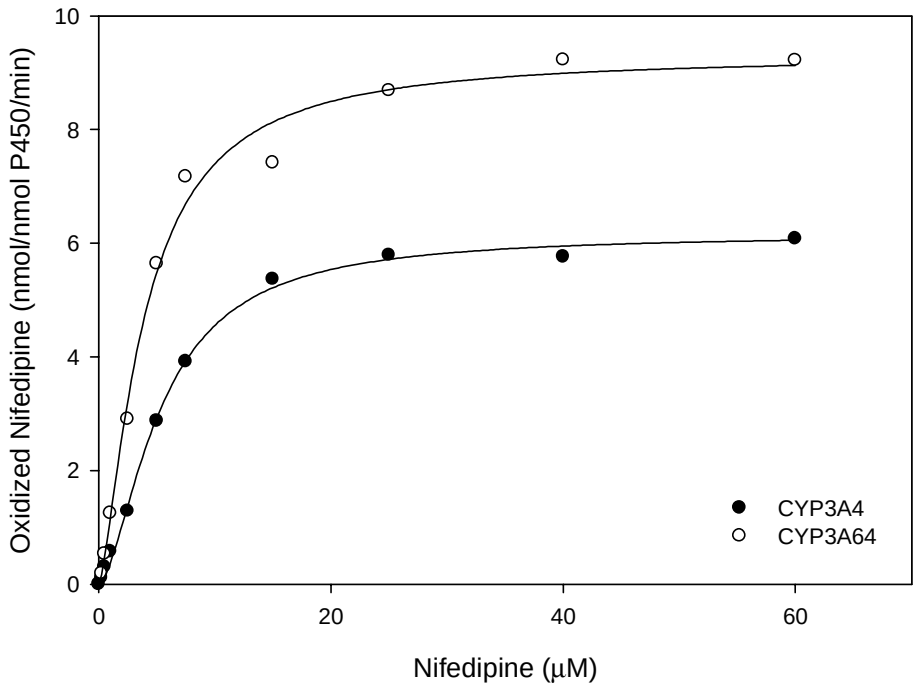

DMD Fast Forward. Published on June 30, 2006 as DOI: 10.1124/dmd.106.009977
This article has not been copyedited and formatted. The final version may differ from this version.

Figure 5

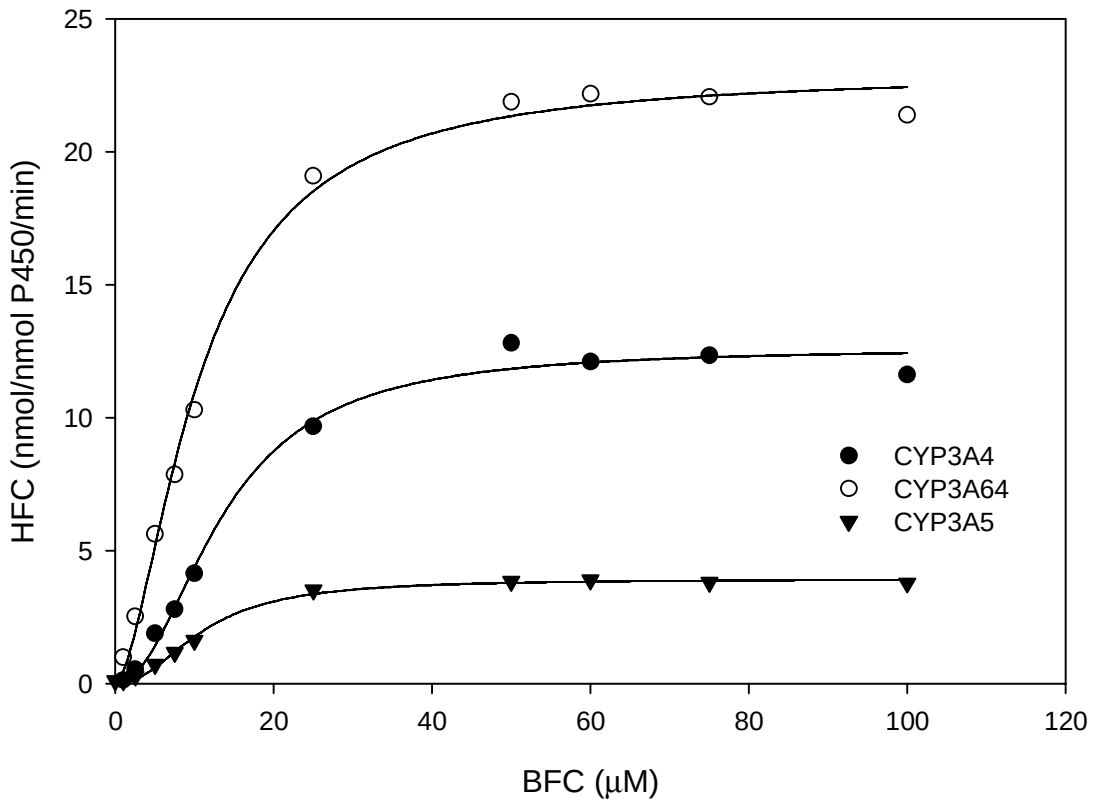

DMD Fast Forward. Published on June 30, 2006 as DOI: 10.1124/dmd.106.009977
This article has not been copyedited and formatted. The final version may differ from this version.

Figure 6

(A)

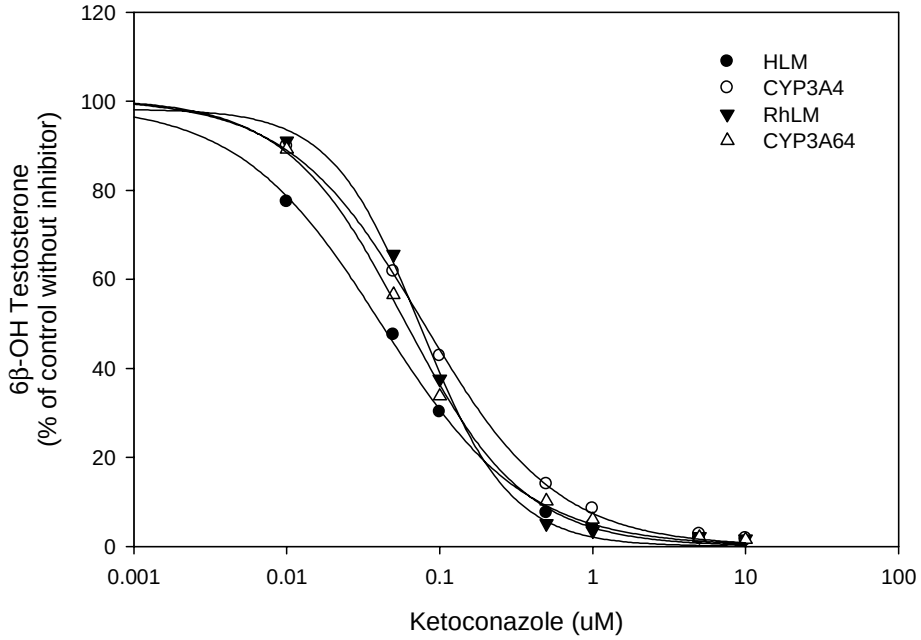

(B)

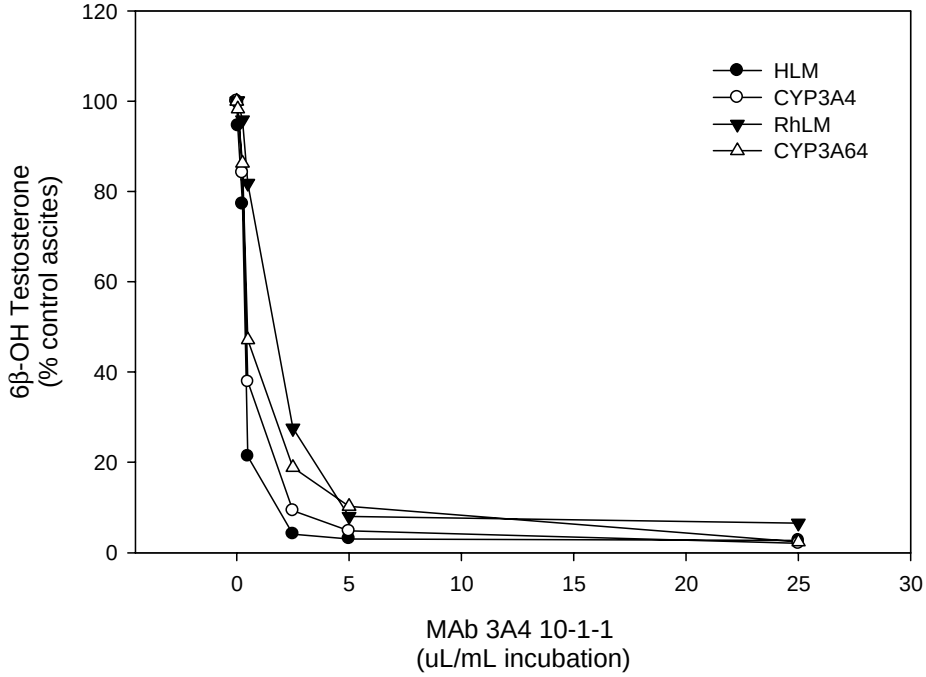

DMD Fast Forward. Published on June 30, 2006 as DOI: 10.1124/dmd.106.009977
This article has not been copyedited and formatted. The final version may differ from this version.

Figure 7

(A)

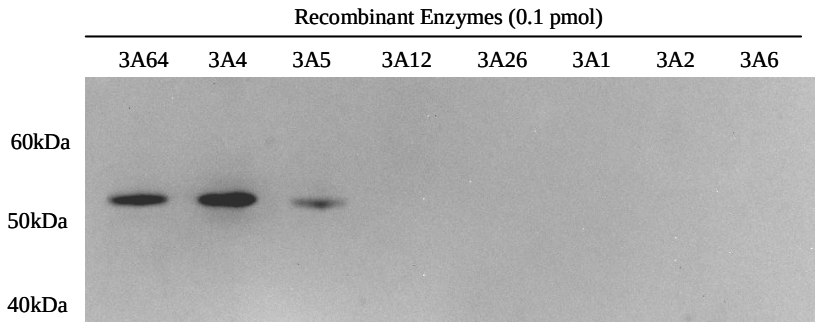

(B)

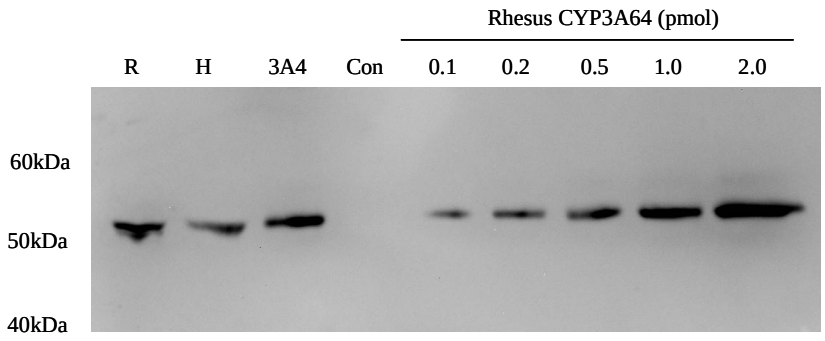

(C)